Neurobiology of Disease 146 (2020) 105137

Contents lists available at ScienceDirect

Neurobiology of Disease

journal homepage: www.elsevier.com/locate/ynbdi

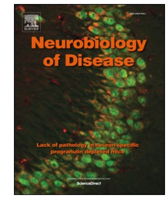

Adenosine A_{2A} receptors format long-term depression and memory strategies in a mouse model of Angelman syndrome

Ana Moreira-de-Sá[a,b], Francisco Q. Gonçalves[a], João P. Lopes[a], Henrique B. Silva[a,b], Ângelo R. Tomé[a,c], Rodrigo A. Cunha[a,b], Paula M. Canas[a,*]

[a] CNC- Center for Neuroscience and Cell Biology, University of Coimbra, 3004-517 Coimbra, Portugal
[b] Faculty of Medicine, University of Coimbra, 3004-504 Coimbra, Portugal
[c] Department of Life Sciences, Faculty of Sciences and Technology, University of Coimbra, 3000-456 Coimbra, Portugal

ARTICLE INFO

Keywords:
Adenosine A_{2A} receptor
Angelman syndrome
Ube3a
Mouse model
Hippocampus
Synaptic plasticity

ABSTRACT

Angelman syndrome (AS) is a neurodevelopmental disorder caused by loss of function of the maternally inherited Ube3a neuronal protein, whose main features comprise severe intellectual disabilities and motor impairments. Previous studies with the *Ube3a*$^{m-/p+}$ mouse model of AS revealed deficits in synaptic plasticity and memory. Since adenosine A_{2A} receptors (A_{2A}R) are powerful modulators of aberrant synaptic plasticity and A_{2A}R blockade prevents memory dysfunction in various brain diseases, we tested if A_{2A}R could control deficits of memory and hippocampal synaptic plasticity in AS.

We observed that *Ube3a*$^{m-/p+}$ mice were unable to resort to hippocampal-dependent search strategies when tested for learning and memory in the Morris water maze; this was associated with a decreased magnitude of long-term depression (LTD) in CA1 hippocampal circuits. There was an increased density of A_{2A}R in the hippocampus of *Ube3a*$^{m-/p+}$ mice and their chronic treatment with the selective A_{2A}R antagonist SCH58261 (0.1 mg/kg/day, ip) restored both hippocampal-dependent learning strategies, as well as LTD deficits.

Altogether, this study provides the first evidence of a role of A_{2A}R as a new prospective therapeutic target to manage learning deficits in AS.

1. Introduction

Angelman syndrome (AS) is a severe neurodevelopmental disorder caused by diverse genetic and epigenetic mechanisms involving the chromosome region 15q11.2-q13, which encodes for the maternally inherited ubiquitin-protein ligase E3A (Ube3a) (Kishino et al., 1997). *Ube3a* controls the ubiquitin proteasome system, ultimately regulating cellular proteostasis (Hamilton and Zito, 2013; Buiting et al., 2016). Since the paternal allele is epigenetically silenced in neurons (Mabb et al., 2011), lack of a maternal contribution results in a nearly complete loss of *Ube3a* function in the brain (Dindot et al. 2008). This underlies the clinical presentation of AS typified by debilitating neurological symptoms such as cognitive deficits, ataxia, speech impairments, abnormal apparent happy demeanour, refractory epilepsy and disruption of sleep patterns (reviewed in Buiting et al., 2016), for which there is no current therapy (Maranga et al., 2020).

New potential therapeutic targets can be identified exploiting *Ube3a* maternal deficient mice (Jiang et al., 1998; Sonzogni et al., 2018), which recapitulate several AS symptoms, including impairments of memory function, deficits of motor performance and abnormal EEGs (Jana, 2012). Their use enabled linking cognitive deficits with compromised hippocampal activity (Jiang et al., 1998; Mardirossian et al., 2009; Maranga et al., 2020) typified by an impairment of neuroplasticity mechanisms, namely of long-term potentiation (LTP) in the hippocampus of *Ube3a*$^{m-/p+}$ mice (Jiang et al., 1998; Sun et al., 2015). Surprisingly, in spite of the increasing recognition of the role of modifications of other forms of synaptic plasticity, namely long-term depression (LTD), for proper memory performance (Connor and Wang,

Abbreviations: A_{2A}R, adenosine A_{2A} receptor; aCSF, artificial cerebrospinal fluid solution; AS, Angelman syndrome; fEPSP, field excitatory post-synaptic potential; HFS, high frequency stimulation; LFS, low frequency stimulation; LTD, long-term depression; LTP, long-term potentiation; mGLUR5, group 5 metabotropic glutamate receptors; MWM, Morris water maze; SCH58261, 7-(2-phenylethyl)-5-amino-2-(2-furyl)-pyrazolo-[4,3-e]-1,2,4-triazolo[1,5 *c*]pyrimidine; *Ube3a*, ubiquitin-protein ligase E3A.

* Corresponding author at: Auxiliary Researcher at Center for Neuroscience and Cell Biology, University of Coimbra, Faculty of Medicine, 1st floor, Rua Larga, 3004-504 Coimbra, Portugal.

E-mail address: canas.paula@gmail.com (P.M. Canas).

https://doi.org/10.1016/j.nbd.2020.105137
Received 5 August 2020; Received in revised form 3 October 2020; Accepted 9 October 2020
Available online 10 October 2020

2016; Temido-Ferreira et al., 2020), barely any information is available regarding putative alterations of LTD in AS.

Reference memory as well as different forms of hippocampal synaptic plasticity are critically dependent on a precise regulation of adenosine A_{2A} receptor ($A_{2A}R$) (reviewed in Cunha, 2016). In fact, the over-functioning of $A_{2A}R$ is critically involved (Laurent et al., 2016; Viana da Silva et al., 2016; Silva et al., 2018) and actually sufficient (Li et al., 2015; Pagnussat et al., 2015; Temido-Ferreira et al., 2020) to disrupt reference memory and hippocampal synaptic plasticity in different neuropsychiatric diseases (reviewed in Cunha, 2016). Thus we now exploited *Ube3a*$^{m-/p+}$ mice to test if $A_{2A}R$ might contribute to AS by exploring if these receptors are upregulated in the hippocampus and if their blockade restores the dysfunction of learning and memory as well as of hippocampal synaptic plasticity in this AS model.

2. Methods

2.1. Animals

Experiments were conducted in 9 weeks old wild-type (WT) and *Ube3a* maternal deficient (*Ube3a*$^{m-/p+}$) mice with a C57BL/6 background originally obtained from The Jackson Laboratory (Bar Harbor, ME, USA; Catalogue Number 016590). Thenceforward, WT males (*Ube3a*$^{m+/p+}$) were crossed with AS female mutants to obtain WT and AS littermates. Mice from both sexes were used for experimental purposes, with animals weighing roughly ~20–25 g. Littermates of the same sex were housed in groups of 2–4 per homecage (NEXT cage, Tecniplast) kept in an environmentally controlled room (22 ± 1 °C, 50 ± 10% relative humidity) on a 12 h light/dark cycle (with lights on at 07:00 a.m.), with both food and water available *ad libitum*. Mice were handled according to the "3R" principles by experienced DGAV/FELASA accredited researchers; in fact, a good example of the application of the "3R" measures was the inclusion of animals from both sexes in the experimental design. Moreover, various actions were taken to reduce animal suffering and/or distress in the course of the behavioural assessments, as it will be further described. All animal experiments were approved by the Ethical Committee of the Center for Neuroscience and Cell Biology of the University of Coimbra (ORBEA n° 138–2016/15072016) and certified by DGAV (the Portuguese National Authority for Animal Health and Well-Being), in accordance with the European Union directive 2010/63/EU for animal experiments.

2.2. Experimental design

To check whether chronic $A_{2A}R$ blockade has an impact on memory performance as well as on synaptic plasticity processes, 9 weeks old WT and AS mice were randomly distributed into groups and daily injected intraperitoneally either with a saline solution (90% NaCl +10% dimethylsulfoxide (DMSO)) or with the $A_{2A}R$ selective antagonist SCH58261 (0.1 mg/kg) for 21 consecutive days, as previously described (Kaster et al., 2015). The SCH58261 (Tocris, Cat. No. 2270, 2018) stock solution was prepared in DMSO and maintained as frozen aliquots at −20 °C. Animals were assigned a number according to their order of birth and, upon genotyping, WT and *Ube3a*$^{m-/p+}$ mice were randomly allocated to a given treatment group (Kim and Shin, 2014). Upon treatment, animals were then subject to a hippocampus-dependent Morris water maze protocol as shown in Fig. 1A. Behavioural experiments were conducted in a blind manner (with the experimenter not knowing the animal genotype and/or treatment group) during the light period of the cycle (between 9 a.m. and 5 p.m.) at approximately the same time each day, to avoid the influence of circadian rhythms on mice performance. Mice were then sacrificed by cervical dislocation followed by decapitation, with the brains being collected for posterior analysis. It is also important to mention that due to the fact that no drugs were administered for the sacrifice, a possible effect in neuronal function which could compromise data interpretation was prevented.

2.3. Morris water maze

Hippocampal-dependent spatial learning and memory was assessed in a standard MWM (Morris et al., 1982), which consisted of a circular pool with a diameter of 105 cm, filled with water (22 ± 1 °C) made opaque with white tempera paint (Giotto; FILA Iberia, Barcelona, Spain). A 10 cm diameter escape platform was submerged approximately 1 cm below the water surface and visual cues were equidistantly placed in the walls around the pool. The protocol was divided into three distinct phases: learning/acquisition stage, retention/probe trial and a visual platform control, as described elsewhere (Vorhees and Williams, 2006; Stanford Behavioural and Functional Neuroscience Laboratory, 2007). After a 1 h acclimatization period to the testing room, mice underwent the learning stage consisting of 4 trials per day with a ~ 20 min intertrial interval, in which mice were placed in different drop locations (randomly generated sequences of the 4 cardinal points across the days) and given 60 s to find the hidden platform. To successfully complete the trial, the animals must remain on the platform for 10 s. This stage is completed when WT SAL mice (control group) escape latency reached an average of 20 s. The probe trial took place 24 h following the last day of training, during which the platform was removed from the pool and each mouse was given 1 min to search for the position of the missing platform (1 single trial from a random drop location). Parameters such as the time spent in the target quadrant, the number of crossings over the location of the missing platform and the type of predominant search strategy (Garthe and Kempermann, 2013) used in each trial were evaluated. Finally, visual and motor acuity of the mice were assessed during a visual platform control trial. In this stage, a visual cue was placed on top of the platform and mice were given 60 s to reach it, from all the four drop locations. In order to minimize animal suffering during the course of this extensive behavioural experiment, mice were gently dried with a heated towel upon leaving the water maze after each trial. The transport cage, where mice that already completed the task were placed, was also over a heating pad. By the end of each training day, animals were closely monitored to assure their well-being. Live videos were recorded and behaviour in the MWM was analysed off-line with Any-Maze version 4.99 tracking software (Stoelting, Wood Dale, USA, Research resource identifier, RRID:SCR_014289).

2.4. Electrophysiological recordings

Upon sacrifice, brains were quickly removed and placed into an ice-cold artificial cerebrospinal fluid solution (aCSF; concentration in mM: 124 NaCl; 3 KCl; 26 $NaHCO_3$; 1.25 NaH_2PO_4; 10 D-glucose; 1 $MgSO_4$; 2 $CaCl_2$) bubbled with a gas mixture of 95% O_2 and 5% CO_2. Extracellular electrophysiological recordings were performed in 400 µm-thick transversal hippocampal slices, made with a McIlwain tissue chopper (RRID:SCR_015798). Individual slices from the dorsal hippocampus were transferred into a resting chamber (Harvard Apparatus, Holliston, USA, Cat. No. PY2 65–0076) and allowed to recover for one hour at either 30.5 °C to induce LTP (Lopes et al., 2015) or at 32.0 °C to induce LTD (Van der Jeugd et al., 2011; Temido-Ferreira et al., 2020; Reis et al., 2019). Test stimuli were applied at 0.05 Hz *via* a Grass S44 square pulse electric stimulator (Grass Instruments, West Warwick, RI, USA) through a concentric bipolar stimulus electrode placed over the Schaffer fibers and the responses were quantified as the maximum slope of the rising phase of the field excitatory post synaptic potentials (fEPSPs) recorded with a glass electrode filled with 4 M NaCl (2–5 MΩ) placed in the CA1 stratum radiatum. The signals were amplified through an ISO-80 amplifier (World Precision Instruments, Herefordshire, UK, Cat. No. ISO-80, 2009) and digitalized through an analogue-digital converter ADC-42 board (Pico Technologies, Pelham, NY, USA). The input/output relation was first determined to evaluate basal transmission (Reis et al., 2019) and to allow selecting the intensity of the stimulus that evoked a fEPSP of approximately 40% of the maximum response for LTP experiments, which was induced with a high-frequency stimulation train (HFS, one single 100 Hz pulse train for 1 s) (Costenla et al., 2011; Lopes et al., 2015); for LTD experiments, a different stimulus intensity was chosen – roughly 60% of the maximal slope – and a low-frequency stimulation protocol was applied (LFS, three trains of 1500

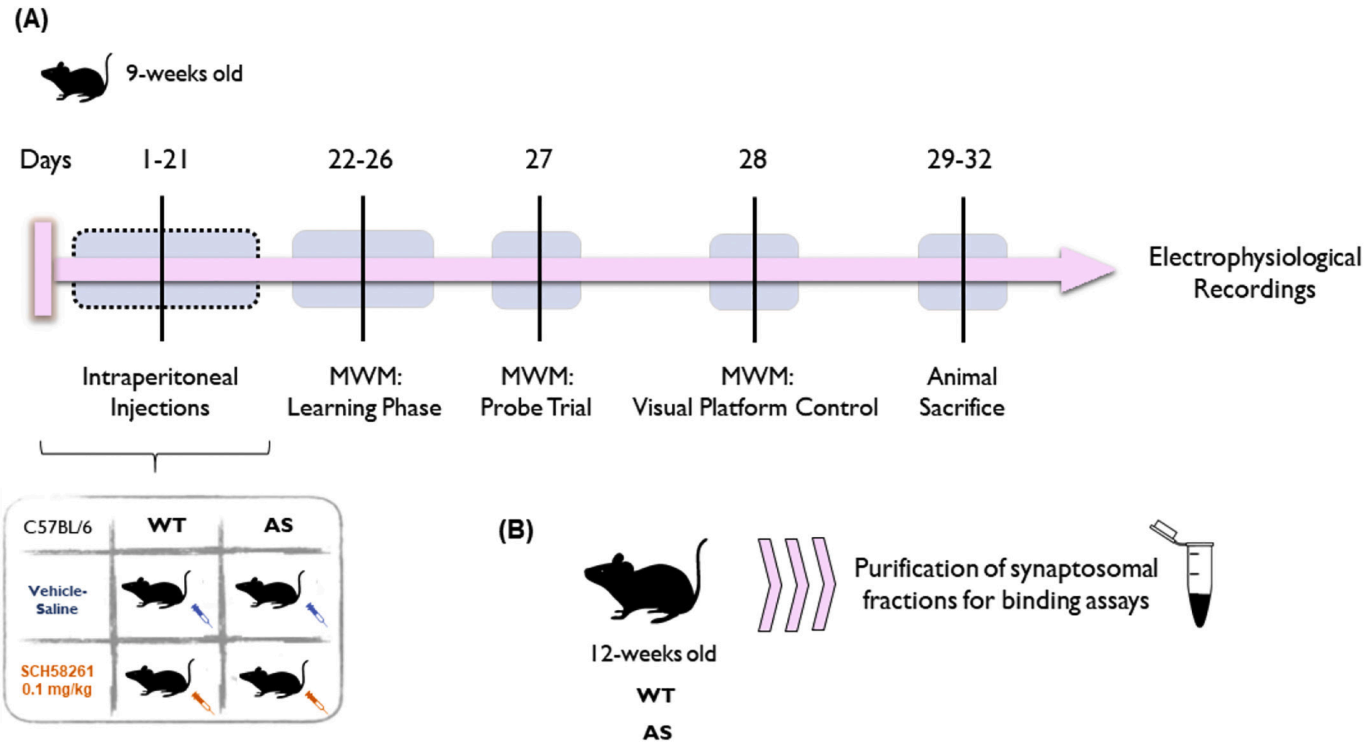

Fig. 1. Study design and timeline of the experimental procedures. (A) Behavioural testing timeline used to assess animals' spatial learning and memory, followed by their sacrifice to carry out electrophysiological recordings in hippocampal slices in order to evaluate synaptic plasticity processes. Additionally, (B) the hippocampi of five naïve animals from each genotype were dissected and used for further neurochemical fractionation and ligand-binding assays.

pulses at 2 Hz, with 10 min of intertrain interval) (Van der Jeugd et al., 2011; Temido-Ferreira et al., 2020; Reis et al., 2019). Both LTP and LTD magnitudes were evaluated by comparing the average of the fEPSP slopes from 50 to 60 min after HFS or LFS induction with the average of the slopes 10 min prior the application of the stimulation protocols and expressed as percentage of change from baseline. In addition, to study the effects of an acute SCH58261 exposure, some control slices from both genotypes were continuously superfused with a supramaximal and selective concentration (50 nM) of this antagonist (Costenla et al., 2011) starting 20 min prior to the delivery of the plasticity-inducing stimulation protocol. The average of every three consecutive fEPSPs traces was stored and the post-synaptic responses were quantified as the maximum slope of the rising phase of the average fEPSPs with the WinLTP 2.20.1 software (RRID:SCR_008590) (Anderson and Collingridge, 2001).

2.5. Synaptosomal preparation

Neurochemical experiments were performed in 5 naïve animals of each genotype (Fig. 1B). Following sacrifice, the hippocampi of each mouse were dissected and homogenised in ice-cold sucrose solution (0.32 M D-sucrose; 1 mM EDTA-Na; 10 mM HEPES; 0.015 mM BSA; pH 7.4 at 4 °C) for subsequent homogenization. To obtain a fraction of purified synapses (*i.e.* synaptosomes), the homogenate was processed through several consecutive differential centrifugation cycles including a 45% Percoll density gradient as previously described (Rebola et al., 2005). The synaptosomal fraction was resuspended in 300 μL of a preincubation solution (50 mM Tris, 1 mM EDTA, 2 mM EGTA, pH 7.4) to determine its protein content with the Bio-Rad protein assay (Bio-Rad, Amadora, Portugal, Cat. No. #5000001, 2017) and stored at −80 °C until used for membrane binding assays.

2.6. Membrane binding assays

Binding assays to estimate $A_{2A}R$ density in synaptosomal membranes were carried out as previously described (Cunha et al., 2006; Reis et al., 2019). Briefly, the synaptosomes were lysed in a Tris/Mg solution (50 mM Tris, 10 mM $MgCl_2$, pH 7.4) and pelleted synaptosomal membranes were incubated for 30 min at 37 °C with adenosine deaminase (2 U/mL; Roche Molecular Biochemicals, Indianapolis, IN, USA, Cat. No. 10102105001, 2018) to remove endogenous adenosine. After centrifugation at 14,000 *g* for 15 min at 4 °C, the pellets were resuspended in 600 μL of Tris/Mg solution with 4 U/mL of adenosine deaminase (Rebola et al., 2005). $A_{2A}R$ binding density was determined with 79–585 μg of synaptosomal membrane protein exposed during 1 h at room temperature to a single supra-maximal concentration (2 nM) of the selective antagonist ^{3}H-SCH58261 (specific activity of 77 Ci/mmol, prepared by GE Healthcare Life Sciences and generously offered by E. Ongini, Schering-Plough, Italy) in a final volume of 200 μL. The binding reactions were stopped by addition of 5 mL of ice-cold Tris/Mg and vacuum filtration through glass fiber filters (Whatman GF/C filters, GE Healthcare Life Sciences, Carnaxide, Portugal), followed by a washing step with 5 mL of ice-cold Tris/Mg. After drying, the filters were placed in vials with 2 mL of scintillation liquid (AquaSafe 500Plus; Zinsser Analytic GMBH, Eschborn, Germany) to measure radioactivity in a 2900TR Tricarb β-counter (PerkinElmer, Lisbon, Portugal). Specific binding was expressed as fmol/mg of protein and determined by subtraction of the non-specific binding, measured in the presence of the mixed A_1/A_{2A} receptor antagonist XAC (Sigma-Aldrich, 2016) at a concentration (12 μM) over a 1000-times higher than that of the radioligands. Total binding measurements were done in triplicates and the nonspecific binding in duplicates. Negative controls in hippocampal membranes of $A_{2A}R$ knockout mice have previously ensured the selectivity of the tested concentration of ^{3}H-SCH58261 (Lopes et al., 2004).

2.7. Statistics

Results are presented as mean ± SEM from n mice (n is the number of mice). No predetermined sample size calculation was performed. Statistical analysis was carried out using the GraphPad Prism 8.1.1. software (San Diego, CA, USA, RRID:SCR_002798). Normality was assessed using Shapiro-Wilk tests. All behavioural and electrophysiological data have been shown to be normally distributed; in what concerns the radioligand binding assay results, the n used was too small to assess normality. Thus, results from the binding assay were analysed with the non-parametric Mann-Whitney test. Single statistical comparisons between two independent experimental groups following a normal distribution were analysed using an unpaired Student's *t*-test, while comparisons between more than two groups were done with either a two- or three-way analysis of variance (ANOVA) for independent means, followed by Tukey's multiple comparisons *post hoc* tests. To classify the search strategy in the MWM, a contingency table was created and a chi-square test of independence was performed in order to test for a possible relationship between the different variables. In addition, when comparing an experimental group sample mean with a pre-defined hypothetical value, a one sample Student's *t*-test was performed. Identification and consequent removal of outliers was made by the Grubb's test. Statistical significance was set for p values < 0.05.

3. Results

3.1. Upregulation of adenosine A_{2A} receptors in hippocampal synapses of AS mice

As illustrated in Fig. 2, binding assays in synaptosomal membranes revealed a significant increase of the density of $A_{2A}R$ in the hippocampus of *Ube3a*$^{m-/p+}$ mice (37.19 ± 1.95 fmol/mg of protein, $n = 5$, $p < 0.05$ with the non-parametric Mann-Whitney test) when compared to their WT littermates (22.33 ± 3.87 fmol/mg of protein, n = 5). The nonspecific binding of the selective $A_{2A}R$ antagonist ^{3}H-SCH58261 was 52.63 ± 10.30% and 62.04 ± 4.57% of total binding in AS and WT mice, respectively. This high percentage of non-specific binding results from the low number of disintegrations per minute (dpm) counts pertaining to the low density of $A_{2A}R$ in the hippocampus. Thus, these data show an upregulation of $A_{2A}R$ in hippocampal synaptic membranes of AS mice.

3.2. AS mice display an altered learning pattern, which is rescued by SCH58261

In light of the cognitive deficits present in AS patients, we evaluated 12-weeks old WT and *Ube3a*$^{m-/p+}$ animals' spatial hippocampal-dependent learning and memory through the MWM task and the impact of the $A_{2A}R$ selective antagonist SCH58261 thereupon (Fig. 1A). As shown in Fig. 3A, mice from all experimental groups (n = 10–16 mice per group) learned the task and improved their performance during the acquisition stage of the protocol (time to reach the platform: WT saline-treated: 46.57 ± 4.08 s in day 1 *vs.* 20.54 ± 2.89 s in day 5; WT SCH58261-treated: 53.04 ± 2.29 s in day 1 *vs.* 21.85 ± 2.75 s in day 5; *Ube3a*$^{m-/p+}$ saline-treated: 50.22 ± 2.55 s in day 1 *vs.* 29.30 ± 3.78 s in day 5; *Ube3a*$^{m-/p+}$ SCH58261-treated: 52.46 ± 1.98 s in day 1 *vs.* 24.67 ± 2.96 s in day 5). A three-way ANOVA did not indicate genotype as a significant source of variation of the mice performance ($F_{1,49} = 3.034$, $p = 0.0878$), and did not identify a significant interaction between genotype and treatment ($F_{1,49} = 0.009177$, $p = 0.9241$); notwithstanding, it is worth noting that only WT saline-treated mice reached the 20 s escape latency pre-defined as the learning criteria by day 5. Regarding the 24 h probe trial, the analysis of the percentage of time that mice spent on the target quadrant in comparison to the other quadrants of the pool, once again showed that all groups seem to have retained the platform location, with all of them spending more than 25% of the trials' time in the target quadrant (% time in target quadrant: WT saline-treated: 43.98 ± 3.86; WT SCH58261-treated: 48.29 ± 5.68; *Ube3a*$^{m-/p+}$ saline-treated: 37.84 ± 3.62; *Ube3a*$^{m-/p+}$ SCH58261-treated: 42.17 ± 3.97; Fig. 3B). Similarly, all groups crossed a similar number of times the exact location of the platform when comparing to the opposite side (% crossings in target platform location: WT saline-treated: 46.79 ± 6.03; WT SCH58261-treated: 48.39 ± 8.39; *Ube3a*$^{m-/p+}$ saline-treated: 36.85 ± 6.37; *Ube3a*$^{m-/p+}$ SCH58261-treated: 43.46 ± 6.46; Fig. 3C), with a two-way ANOVA analysis not revealing any significant interactions or statistical differences of the number of crossings in the target location according to genotype ($p = 0.2959$) and/or treatment ($p = 0.5620$). We also did not find any significant differences in behavioural data analysis with respect to sex within genotypes in neither of the distinct stages (data now shown). Furthermore, WT and AS mice found equally well the cued visible platform in the visual control trial, with all groups reaching the platform in less than 15 s regardless of the treatment, and no major differences were found between the maximum swimming speed of the experimental groups (data now shown); thus, motor alterations do not seem to negatively impact AS animals' performance in a significant manner. Altogether, these findings point towards an apparent lack of pronounced spatial learning and memory deficits in AS mice, based on the parameters so far evaluated in the MWM task.

We next analysed the overall search patterns of the mice attempting to find the hidden platform during the retention trial. We classified strategies either as hippocampus-dependent (allocentric) or not hippocampus-dependent (egocentric), as previously described (Garthe and Kempermann, 2013). As seen in Fig. 4, although *Ube3a*$^{m-/p+}$ saline-treated mice were able to find the hidden platform, they appear to be the only experimental group that preferentially resorted to non-hippocampal strategies (with only 37.5% of mice searching in a hippocampus-dependent manner out of a total of 16 mice). Remarkably, treatment with SCH58261 reverted this pattern (66.67% of *Ube3a*$^{m-/p+}$ SCH58261-treated mice now resorted to the hippocampus to find the hidden platform location, while the remaining 33.33% used a hippocampus-independent strategy, out of a total of 15 mice). Indeed, a chi-square test of independence showed a significant relationship between the animals' genotype and treatment and their capability to resort to the hippocampus in order to find the hidden platform location $X^2(3, N = 53) = 7.995$, $p = 0.0461$. Notably, the reported phenotype does not rely on the sex of the animals (Supplementary Fig. 1), which is in agreement with current data showing that such differences do not influence *Ube3a*$^{m-/p+}$ animals' performance in the Morris Water Maze task (Koyavski et al., 2019).

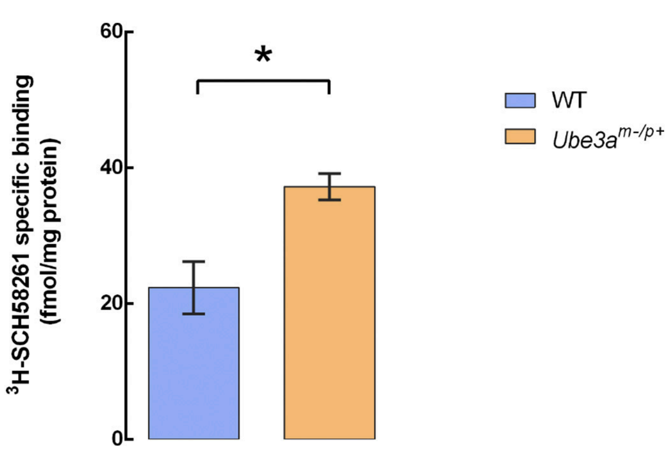

Fig. 2. Adenosine A_{2A} receptor density is markedly increased in hippocampal synaptosomal membranes of *Ube3a* maternal-deficient (*Ube3a*$^{m-/p+}$) mice modelling Angelman syndrome. Membrane binding assays were performed resorting to a supra-maximal and selective concentration of the A_{2A} receptor antagonist ^{3}H-SCH58261 (2 nM), n = 5 per group, *p < 0.05, Mann-Whitney test.

3.3. *Ube3a*$^{m-/p+}$ mice display impaired hippocampal long-term depression

Synaptic plasticity processes, namely LTP and LTD, are the best candidate processes underlying the processing of persistent memory traces and in the acquisition of cognitive navigation maps (Shapiro,

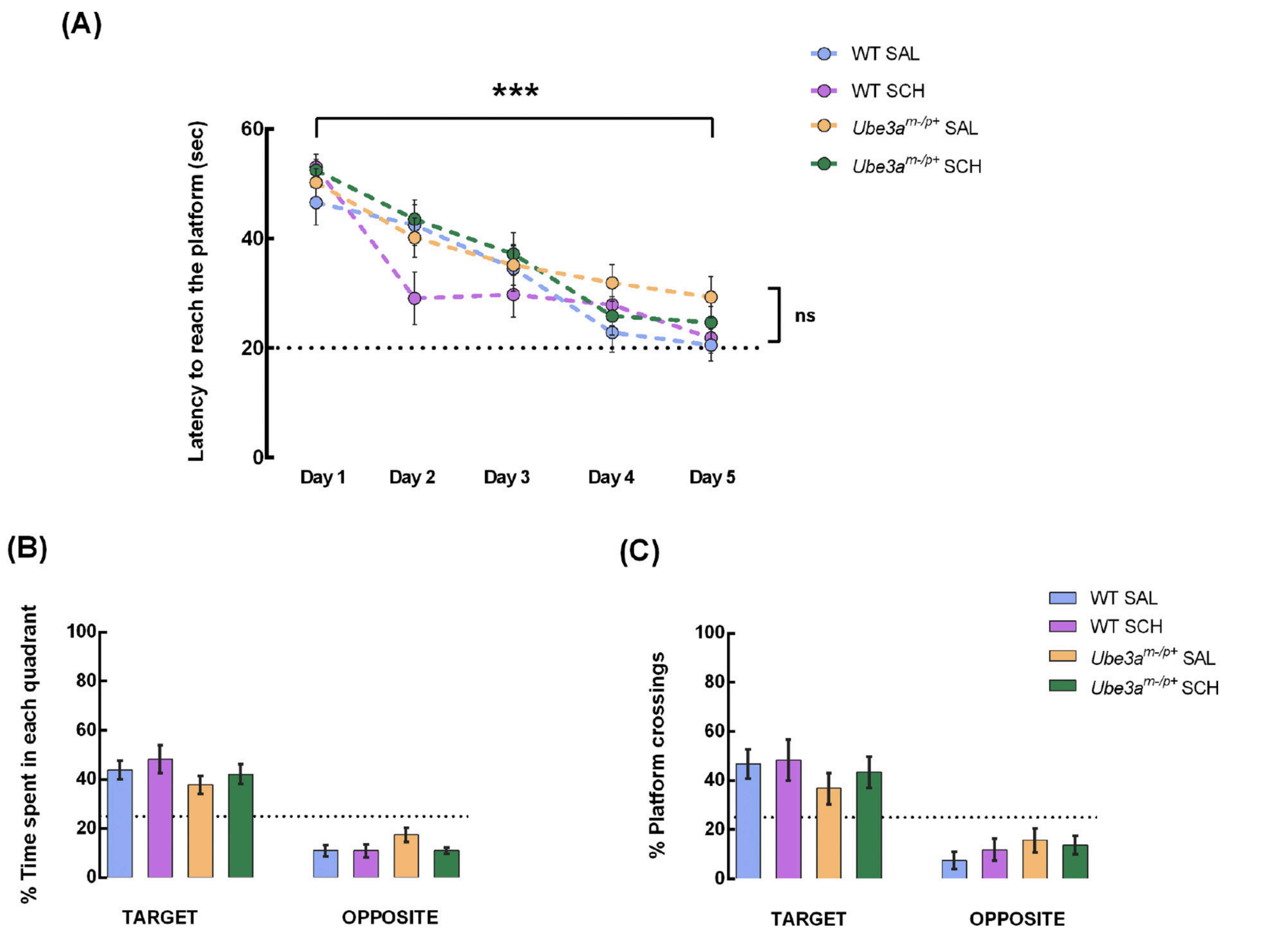

Fig. 3. *Ube3a* maternal-deficient (*Ube3a*$^{m-/p+}$) mice modelling Angelman syndrome do not appear to have neither pronounced learning nor memory impairments, as concluded from their overall performance in the Morris water maze task. (A) Acquisition learning curve. (B) Percentage of time spent in the target quadrant and (C) percentage of crossings in the retention probe trial of saline- and SCH58261-treated animals (WT SAL, $n = 10$; WT SCH, $n = 12$; *Ube3a*$^{m-/p+}$ SAL, $n = 16$; *Ube3a*$^{m-/p+}$ SCH, $n = 15$). *** $p < 0.001$, three-way ANOVA followed by Tukey's multiple comparisons *post hoc* test for the factor time.

2001; Fedulov et al., 2007; Connor and Wang, 2016). Since *Ube3a*$^{m-/p+}$ mice appear to have some difficulties to resort to the hippocampus in order to carry out the MWM task, we decided to check for hippocampal alterations in the aforementioned synaptic plasticity processes. Recordings in Schaffer fiber-CA1 pyramidal synapses did not reveal significant alterations in basal transmission, with similar input/output curves in WT and AS littermates (Fig. 5A). Also, we did not detect changes in LTP profile and magnitude (41.89 ± 9.96% of change over baseline in *Ube3a*$^{m-/p+}$ mice *vs.* 46.77 ± 10.02% of potentiation in WT, Fig. 5B and C). In contrast, LTD was significantly decreased in hippocampal slices of AS mice (−2.88 ± 5.22% *vs.* -17.71 ± 4.31% of baseline change in WT, $p = 0.0459$, unpaired Student's *t*-test, Fig. 5D and E). Thus, *Ube3a*$^{m-/p+}$ mice might have problems to engage hippocampal LTD processes compared to WT animals.

3.4. Both acute and chronic exposure to SCH58261 rescues LTD in AS mice

Since $A_{2A}R$ overfunction triggers LTD deficits (Laurent et al., 2016; Temido-Ferreira et al., 2020) and $A_{2A}R$ are upregulated in hippocampal synapses of AS mice, we next evaluated if SCH58261 can restore the LTD impairment in AS mice. Fig. 6A and B show that the acute incubation of slices with SCH58261 recovered LTD induction in *Ube3a*$^{m-/p+}$ mice (−20.41 ± 7.26% of baseline, $n = 8$; $p = 0.0261$ using a one sample *t*-test *vs.* 0%) to values close to these found in slices from WT mice, with overlapping time-course profiles (in green and light blue, respectively, in Fig. 6A). Acute SCH58261 treatment of slices from WT mice also afforded a robust LTD magnitude (−32.70 ± 3.53% of baseline, n = 8). A two-way ANOVA revealed a significant effect of both genotype ($p = 0.0156$) and treatment ($p = 0.0045$) in LTD magnitude.

We confirmed this alteration of $A_{2A}R$-mediated control of LTD in chronically SCH58261-treated *Ube3a*$^{m-/p+}$ mice (Fig. 1A). No differences were found in the input/output curves irrespective of treatment (Fig. 6C). However, when inducing LTD with a LFS protocol, chronic $A_{2A}R$ blockade ameliorated the marked magnitude deficits detected in AS mice (−14.55 ± 5.91% of baseline change in *Ube3a*$^{m-/p+}$ SCH59261-treated mice; $p = 0.0432$ with a one sample *t*-test *vs.* 0%, showing that LTD was successfully engaged; Fig. 6D and E).

4. Discussion

The present study provides, to the best of our knowledge, the first evidence of a role of adenosine A_{2A} receptors ($A_{2A}R$) in the impairment of both cognitive and synaptic plasticity processes in *Ube3a*$^{m-/p+}$ mice modelling Angelman syndrome (AS mice).

We began by demonstrating that the density of $A_{2A}R$ was increased in hippocampal synapses of AS mice, in a manner similar to what occurs in several other neuropsychiatric disorders involving deficits of memory performance (reviewed in Cunha, 2016). We cannot discard the possibility that $A_{2A}R$ density might also be altered in extra-synaptic compartments such as in glia cells (Matos et al., 2012), although this should not mask the increased density observed in synaptosomal preparations that display less than 2% of glia contaminants (Cunha et al. 1992; Rodrigues et al. 2008; Quiroz et al. 2009). We next attempted to detail alterations of learning and memory performance and of hippocampal

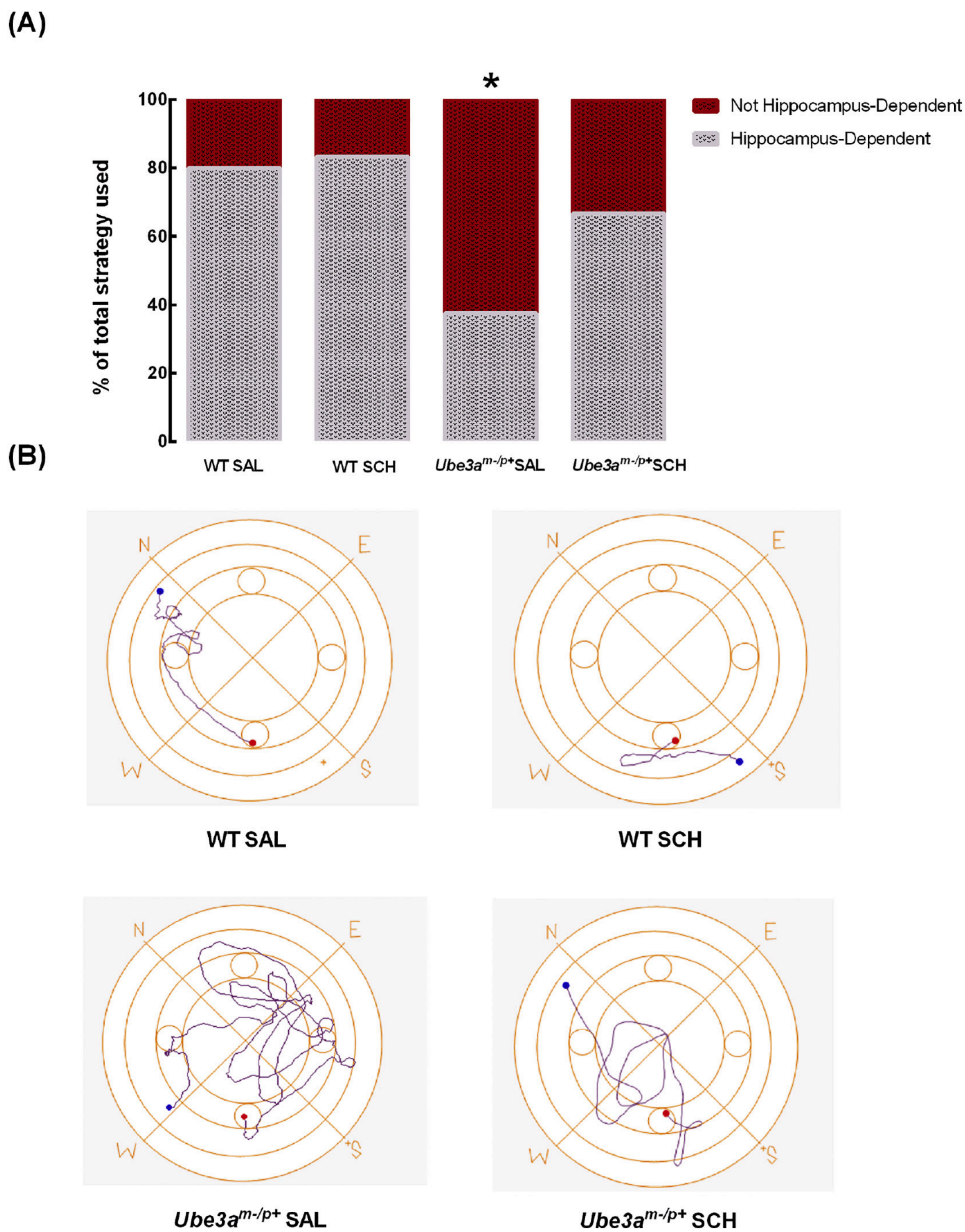

Fig. 4. Search strategy patterns used by rodents to discover the hidden platform location in the Morris water maze probe trial. (A) *Ube3a* maternal-deficient (*Ube3a*$^{m-/p+}$) mice modelling Angelman syndrome treated with the saline solution across the 21 days appear to be the only experimental group which preferentially resorted to strategies that do not implicate the use of the hippocampus (classified as "unspatial") to find the hidden platform in the probe trial of the test. *$p < 0.05$, chi-square test of independence, n = 10–16 mice per group. (B) Representative images of the search patterns employed by animals during the course of the probe trial for each experimental group.

synaptic plasticity to directly test the hypothesis that $A_{2A}R$ overfunction might be a causative factor for the expression of cognitive symptoms in AS. We explored performance in the Morris water maze (MWM) since it allows probing hippocampal-dependent learning and memory functions (Morris et al., 1982) and we started using mice at 9 weeks of age, a time when others reported the emergence of learning and memory dysfunction in *Ube3a*$^{m-/p+}$ mice (van Woerden et al., 2007; Huang et al., 2013; Sun et al., 2015). However, our data did not reveal any significant differences between age-matched WT and *Ube3a*$^{m-/p+}$ mice in any of the different stages of the MWM protocol. Indeed, strain, age, genetic background-dependent differences and even alterations in the intertrial interval duration have been proposed to result in conflicting reports regarding the performance of the *Ube3a*$^{m-/p+}$ mouse in this MWM task (Huang et al., 2013; Sonzogni et al., 2018). Furthermore, it is important to note that another possible meddling factor influencing animals' performance in the MWM might be the phase of the light-dark cycle in which *Ube3a* maternal deficient mice fulfil the task, since there are some controversial reports on a possible impairment of the circadian clock rhythmicity in this model (Shi et al. 2015, Ehlen et al. 2015). We then decided to detail the performance in the MWM, searching for differences in the overall exploratory patterns of mice in the probe trial, which can inform on the recruitment of hippocampal or non-hippocampal pathways

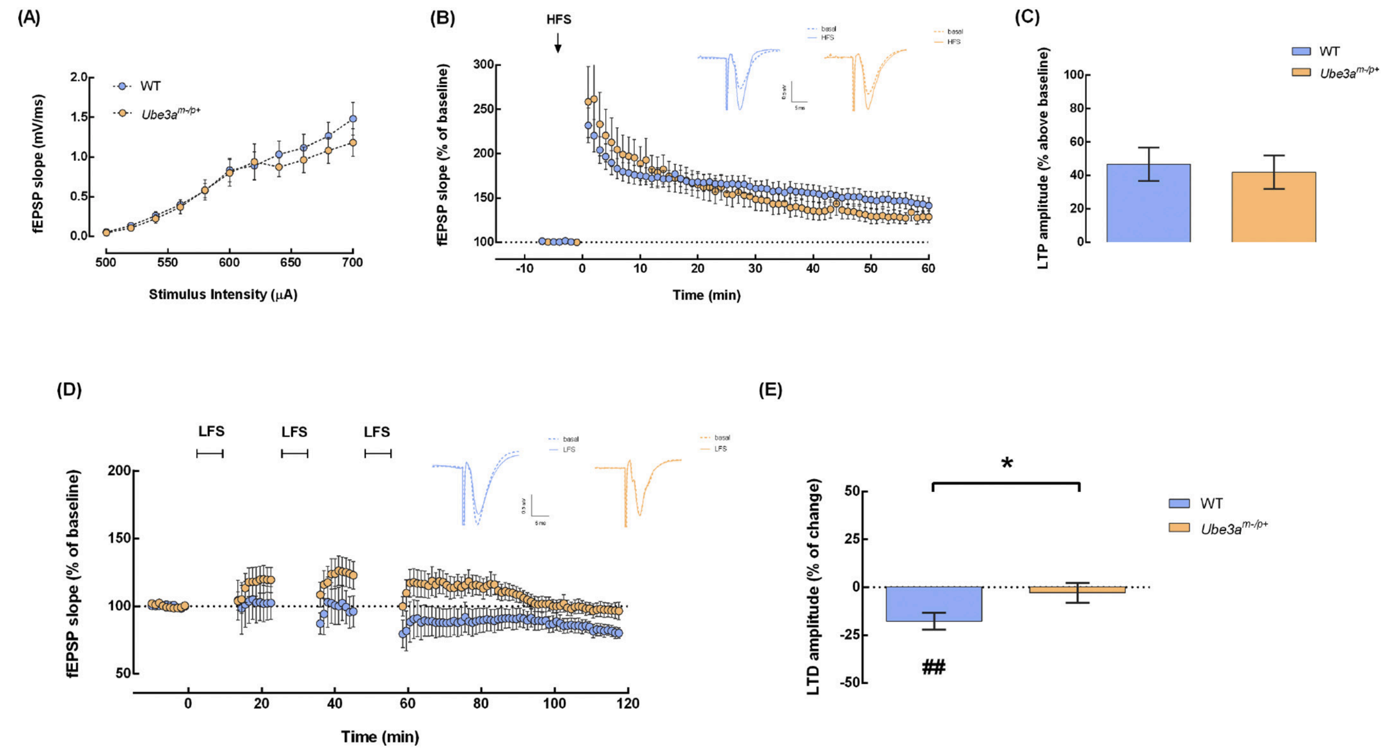

Fig. 5. *Ube3a* maternal-deficient ($Ube3a^{m-/p+}$) mice modelling Angelman syndrome exhibit deficits in hippocampal synaptic LTD-like plasticity processes. Electrophysiological recordings were performed in hippocampal slices of 12-weeks old WT ($n = 8$) and $Ube3a^{m-/p+}$ mice (n = 8). (A) Basal neuronal transmission did not differ among genotypes, as concluded by the lack of alteration of input/output curves. (B) Time-course changes of the fEPSP slope (expressed as percentage of baseline values) upon applying an high-frequency (HSF) train (100 Hz for 1 s) in the CA1 hippocampal region; the inserts show representative recordings of the fEPSPs obtained for both WT (blue) and AS mice (orange) prior to LTP induction (dashed traces) and in the last 10 min of the experiment (filled lines). (C) Bar graph showing similar LTP magnitude in WT and AS mice. (D) Time course of LTD induction by low frequency trains (LFS, 3 trains of 1500 pulses at 2 Hz applied for 10 min each, with 10 min of intertrain interval) in WT and AS mice, which magnitudes are presented in the bar graph (E). *$p < 0.05$, unpaired Student's *t*-test. ## $p < 0.01$, one sample *t*-test comparing the mean value of the group with the hypothetical value of zero. (For interpretation of the references to colour in this figure legend, the reader is referred to the web version of this article.)

to resolve the task (Garthe and Kempermann, 2013). In fact, the analysis of the spatial search strategy might provide more sophisticated insights into the dynamic nature of cognition employed to resolve the MWM (Rogers et al., 2017), which has previously allowed a distinction of the performance of animals with similar overall scoring in the MWM based on the analysis of their swimming paths classified as either hippocampus-dependent (allocentric navigation, independent of self) or not hippocampus-dependent (egocentric strategies, self-centred) (Grech et al., 2018). With progressive training in the MWM, healthy animals are expected to integrate the egocentric route-knowledge into an allocentric representation (Garthe and Kempermann, 2013). Remarkably, we found that most $Ube3a^{m-/p+}$ mice were not able to resort to spatial allocentric search strategies in order to find the hidden platform, thus indicating a potential deficit in hippocampal functioning and cognitive map formation. By contrast, SCH58261-treated $Ube3a^{m-/p+}$ mice displayed a clear preference for hippocampus-dependent search strategies, thus suggesting a possible role of $A_{2A}R$ blockade in the amelioration of hippocampal-associated cognitive deficits. This is in global agreement with the previously reported ability of $A_{2A}R$ overfunction to deteriorate hippocampal-dependent memory performance (Li et al., 2015; Pagnussat et al., 2015; Temido-Ferreira et al., 2020) and conversely, with the ability of $A_{2A}R$ blockade to recover memory performance in different neuropsychiatric conditions (Kaster et al., 2015; Laurent et al., 2016; Viana da Silva et al., 2016; Silva et al., 2018; Temido-Ferreira et al., 2020).

Finally, we explored if this behavioural alteration of performance in the MWM was associated with alterations of hippocampal synaptic plasticity, which have been argued to represent the neurophysiological basis of learning and memory (Shapiro, 2001). We now report that *Ube3a* maternal deficient mice have difficulties in engaging LTD mechanisms upon LFS stimulation of Schaffer collateral fibers. These deficits of LTD in $Ube3a^{m-/p+}$ mice appear to be selective since it was not accompanied by differences in either basal synaptic transmission or LTP induction with a HFS protocol in hippocampal slices from $Ube3a^{m-/p+}$ mice. This lack of alteration of LTP is at odds with the previous description of an impaired LTP consolidation in the CA1 field of AS mice (Baudry et al., 2012; Sun et al., 2016; Liu et al., 2019) and probably results either from the use of different induction protocols (the aforementioned authors resort to theta-burst stimulation, while we applied a classical HFS protocol that we know to be controlled by $A_{2A}R$; see *e.g.* (Lopes et al., 2015)) or from the use of $Ube3a^{m-/p+}$ mice with a different extent of learning and memory impairment (as discussed above). The presently observed LTD deficit in $Ube3a^{m-/p+}$ mice provides a compelling neurophysiological basis for the deficits of hippocampal-dependent search strategy in the MWM by $Ube3a^{m-/p+}$ mice, in view of the increasingly recognized role of LTD mechanisms in operations involving hippocampal-dependent learning and memory (Van der Jeugd et al., 2011).

In accordance with the ability of SCH58261 to recover the deficient hippocampal-dependent searching strategy in $Ube3a^{m-/p+}$ mice, we also observed that SCH58261 was able to recover the deficient LTD induction in hippocampal slices from $Ube3a^{m-/p+}$ mice. This is in agreement with previous observations that both chronic and acute pharmacological $A_{2A}R$ blockade could recover deficits of hippocampal LTD associated with the disruption of spatial reference memory in animal models of ageing or Alzheimer's disease (Laurent et al., 2016; Mouro et al., 2017; Temido-Ferreira et al., 2020). The impact of $A_{2A}R$ on synaptic plasticity and memory performance in $Ube3a^{m-/p+}$ mice may eventually involve a rebalance of either proteostasis, known to control memory performance (Jarome and Devulapalli, 2018) and to be

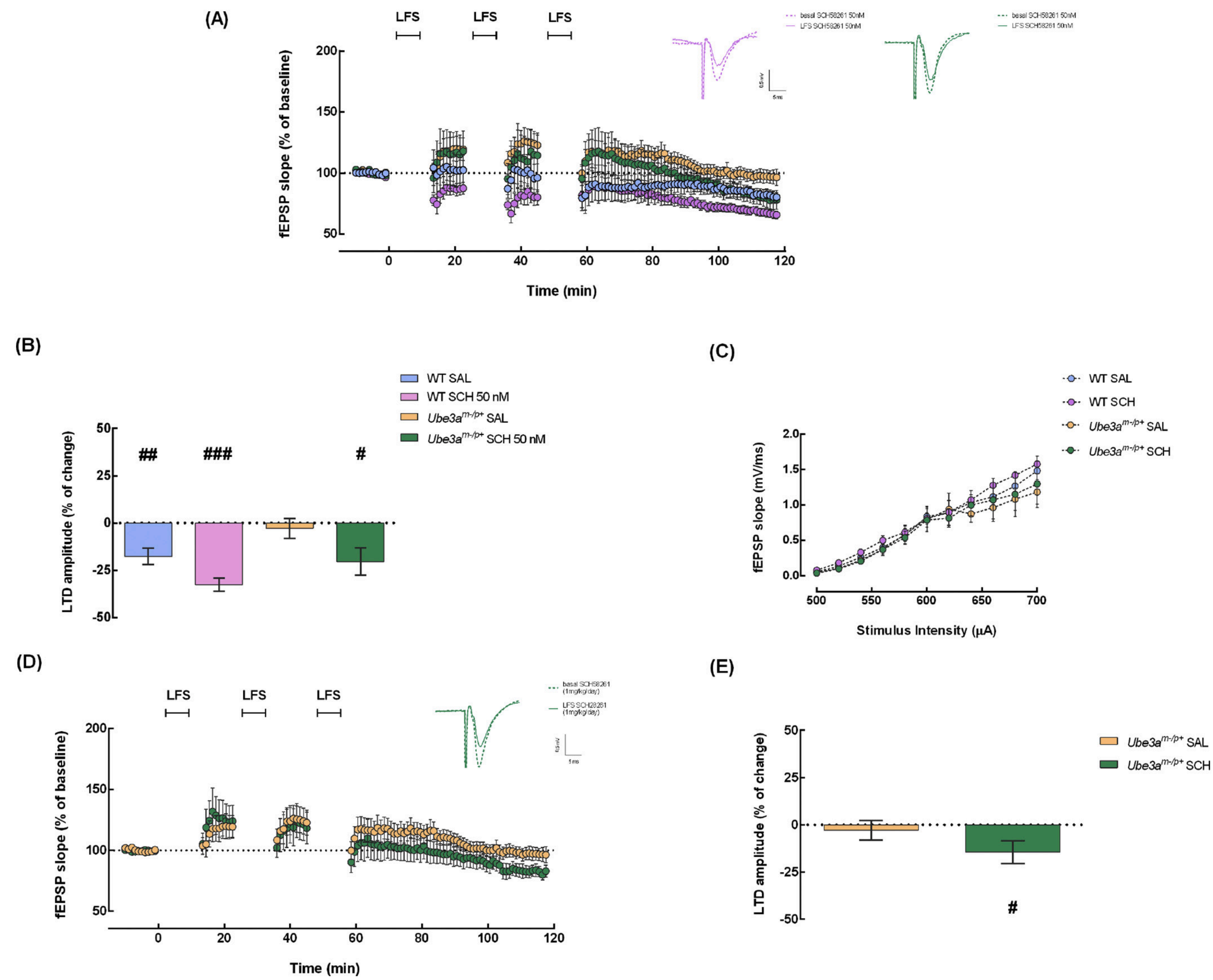

Fig. 6. Pharmacological blockade of $A_{2A}R$ prevents the LTD impairments found in hippocampal slices of *Ube3a* maternal-deficient (*Ube3a*$^{m-/p+}$) mice modelling Angelman syndrome. (A,B) Effects of an acute exposure of hippocampal slices to the $A_{2A}R$ selective antagonist SCH58261 (50 nM) upon low frequency stimulation (LFS) induction of LTD in a time-course graph (A) and in a bar graph (B) summarizing LTD magnitudes in the distinct experimental groups. (C) Extracellular recordings of fEPSP in the CA1 region did not reveal any effect of SCH58261 in the input/output curves. (D,E) In a similar way to what happens upon acute incubation of hippocampal slices with SCH58261, the prolonged intraperitoneal injection of the $A_{2A}R$ antagonist also abrogated LTD deficits in *Ube3a*$^{m-/p+}$ mice. (D) Time course of LFS-induced LTD in *Ube3a*$^{m-/p+}$ mice without or with SCH58261 (0.1 mg/kg/day) treatment; the insert shows representative recordings of fEPSPs in both baseline condition (dashed line) and after LTD induction (filled line) in slices from *Ube3a*$^{m-/p+}$ mice treated with SCH58261 (0.1 mg/kg/day). (E) Average LTD magnitude in *Ube3a*$^{m-/p+}$ mice, showing the ability of SCH58261 treatment to recover LTD magnitude. Data are mean ± SEM of n independent experiments, with n representing the number of animals used per group – WT SAL, n = 8; WT SCH 50 nM, n = 8; *Ube3a*$^{m-/p+}$ SAL, n = 8; *Ube3a*$^{m-/p+}$ SCH 50 nM, n = 8; *Ube3a*$^{m-/p+}$ SCH58261-treated, $n = 9$. One outlier was removed from the *Ube3a*$^{m-/p+}$ chronic SCH58261 treatment group by the Grubb's test. # $p < 0.05$, ## $p < 0.01$, ### $p < 0.001$, one sample *t*-test comparing the mean value of a given experimental group with the hypothetical value of zero.

affected in AS (Mabb et al., 2011; Jana, 2012) and by $A_{2A}R$ (Chiang et al., 2009), or the c-Jun-N-terminal-Kinase (JNK) stress pathway, known to control memory performance (Coffey, 2014) and to be altered in AS (Musi et al., 2020) and by $A_{2A}R$ (Schulte and Fredholm, 2003; Canas et al., 2009; Cunha, 2016), or even the function of group 5 metabotropic glutamate receptors (mGluR5), which control memory performance (Ménard and Quirion, 2012), are a known substrate of the Ube3a protein (Sell and Margolis, 2015) and tightly interact with $A_{2A}R$ (Temido-Ferreira et al., 2020). Although the exact pathways involved in the beneficial outcomes resulting from the pharmacological blockade of $A_{2A}R$ in AS still require additional experimental efforts to be defined, the present findings provide the first evidence for a role of $A_{2A}R$ overfunction in the mechanisms of disruption of hippocampal synaptic plasticity and hippocampal-dependent memory performance in AS mice and reinforce the proposal that hippocampal LTD processes may constitute a neurophysiological basis of hippocampal-dependent memory performance.

Acknowledgements, funding and disclosure of conflicts of interest

This research work was supported by Fundação Amélia de Mello (Bolsa Pedro Maria José de Mello Costa Duarte, 2017), Centro 2020 (CENTRO-01-0145-FEDER-000008:BrainHealth 2020 and CENTRO-01-0246-FEDER-000010) and Fundação para a Ciência e Tecnologia (FCT, POCI-01-0145-FEDER-031274 and UIDB/04539/2020). The funding sources were not involved in the study design, data collection, analysis or preparation of the manuscript. RA Cunha is a scientific consultant of the Institute for Scientific Information on Coffee (ISIC). All other

authors declare no competing financial interests. All experiments were conducted in compliance with the ARRIVE guidelines.

Appendix A. Supplementary data

Supplementary data to this article can be found online at https://doi.org/10.1016/j.nbd.2020.105137.

References

Anderson, W.W., Collingridge, G.L., 2001. The LTP program: a data acquisition program for on-line analysis of long-term potentiation and other synaptic events. J. Neurosci. Methods 108, 71–83. https://doi.org/10.1016/s0165-0270(01)00374-0.

Baudry, M., Kramar, E., Xu, X., Zadran, H., Moreno, S., Lynch, G., Gall, C., Bi, X., 2012. Ampakines promote spine actin polymerization, long-term potentiation, and learning in a mouse model of Angelman syndrome. Neurobiol. Dis. 47, 210–215. https://doi.org/10.1016/j.nbd.2012.04.002.

Buiting, K., Williams, C., Horsthemke, B., 2016. Angelman syndrome - insights into a rare neurogenetic disorder. Nat. Rev. Neurol. 12, 584–593. https://doi.org/10.1038/nrneurol.2016.133.

Canas, P.M., Porciúncula, L.O., Cunha, G.M., Silva, C.G., Machado, N.J., Oliveira, J.M., Oliveira, C.R., Cunha, R.A., 2009. Adenosine A_{2A} receptor blockade prevents synaptotoxicity and memory dysfunction caused by beta-amyloid peptides via p38 mitogen-activated protein kinase pathway. J. Neurosci. 29, 14741–14751. https://doi.org/10.1523/JNEUROSCI.3728-09.2009.

Chiang, M.C., Chen, H.M., Lai, H.L., Chen, H.W., Chou, S.Y., Chen, C.M., Tsai, F.J., Chern, Y., 2009. The A_{2A} adenosine receptor rescues the urea cycle deficiency of Huntington's disease by enhancing the activity of the ubiquitin-proteasome system. Hum. Mol. Genet. 18, 2929–2942. https://doi.org/10.1093/hmg/ddp230.

Coffey, E.T., 2014. Nuclear and cytosolic JNK signalling in neurons. Nat. Rev. Neurosci. 15, 285–299. https://doi.org/10.1038/nrn3729.

Connor, S.A., Wang, Y.T., 2016. A place at the table: LTD as a mediator of memory genesis. Neuroscientist 22, 359–371. https://doi.org/10.1177/1073858415588498.

Costenla, A.R., Diógenes, M.J., Canas, P.M., Rodrigues, R.J., Nogueira, C., Maroco, J., Agostinho, P.M., Ribeiro, J.A., Cunha, R.A., de Mendonça, A., 2011. Enhanced role of adenosine A_{2A} receptors in the modulation of LTP in the rat hippocampus upon ageing. Eur. J. Neurosci. 34, 12–21. https://doi.org/10.1111/j.1460-9568.2011.07719.x.

Cunha, R.A., Sebastião, A.M., Ribeiro, J.A., 1992. Ecto-5'-nucleotidase is associated with cholinergic nerve terminals in the hippocampus but not in the cerebral cortex of the rat. J Neurochem. 59, 657–666. https://doi.org/10.1111/j.1471-4159.1992.tb09420.x.

Cunha, R.A., 2016. How does adenosine control neuronal dysfunction and neurodegeneration? J. Neurochem. 139, 1019–1055. https://doi.org/10.1111/jnc.13724.

Cunha, G.M., Canas, P.M., Oliveira, C.R., Cunha, R.A., 2006. Increased density and synapto-protective effect of adenosine A_{2A} receptors upon sub-chronic restraint stress. Neuroscience 141, 1775–1781. https://doi.org/10.1016/j.neuroscience.2006.05.024.

Dindot, S.V., Antalffy, B.A., Bhattacharjee, M.B., Beaudet, A.L., 2008. The Angelman syndrome ubiquitin ligase localizes to the synapse and nucleus, and maternal deficiency results in abnormal dendritic spine morphology. Hum Mol Genet. 17, 111–118. https://doi.org/10.1093/hmg/ddm288.

Ehlen, J.C., Jones, K.A., Pinckney, L., Gray, C.L., Burette, S., Weinberg, R.J., Evans, J.A., Brager, A.J., Zylka, M.J., Paul, K.N., Philpot, B.D., DeBruyne, J.P., 2015. Maternal Ube3a Loss Disrupts Sleep Homeostasis But Leaves Circadian Rhythmicity Largely Intact. J Neurosci. 35, 13587–13598. https://doi.org/10.1523/JNEUROSCI.2194-15.2015.

Fedulov, V., Rex, C.S., Simmons, D.A., Palmer, L., Gall, C.M., Lynch, G., 2007. Evidence that long-term potentiation occurs within individual hippocampal synapses during learning. J. Neurosci. 27, 8031–8039. https://doi.org/10.1523/JNEUROSCI.2003-07.2007.

Garthe, A., Kempermann, G., 2013. An old test for new neurons: refining the Morris water maze to study the functional relevance of adult hippocampal neurogenesis. Front. Neurosci. 7, 63. https://doi.org/10.3389/fnins.2013.00063.

Grech, Adrienne, Nakamura, Jay, Hill, Rachel, 2018. The importance of distinguishing allocentric and egocentric search strategies in rodent hippocampal-dependent spatial memory paradigms: getting more out of your data. In: The Hippocampus - Plasticity and Functions, https://doi.org/10.5772/intechopen.76603.

Hamilton, A.M., Zito, K., 2013. Breaking it down: the ubiquitin proteasome system in neuronal morphogenesis. Neural. Plast. https://doi.org/10.1155/2013/196848. e9842.

Huang, H.S., Burns, A.J., Nonneman, R.J., Baker, L.K., Riddick, N.V., Nikolova, V.D., Riday, T.T., Yashiro, K., Philpot, B.D., Moy, S.S., 2013. Behavioral deficits in an Angelman syndrome model: effects of genetic background and age. Behav. Brain Res. 243, 79–90. https://doi.org/10.1016/j.bbr.2012.12.052.

Jana, N.R., 2012. Understanding the pathogenesis of Angelman syndrome through animal models. Neural. Plast. 2012, 710943. https://doi.org/10.1155/2012/710943.

Jarome, T.J., Devulapalli, R.K., 2018. The ubiquitin-proteasome system and memory: moving beyond protein degradation. Neuroscientist 24, 639–651. https://doi.org/10.1177/1073858418762317.

Jiang, Y.H., Armstrong, D., Albrecht, U., Atkins, C.M., Noebels, J.L., Eichele, G., Sweatt, J.D., Beaudet, A.L., 1998. Mutation of the Angelman ubiquitin ligase in mice causes increased cytoplasmic p53 and deficits of contextual learning and long-term potentiation. Neuron 21, 799–811. https://doi.org/10.1016/S0896-6273(00)80596-6.

Kaster, M.P., Machado, N.J., Silva, H.B., Nunes, A., Ardais, A.P., Santana, M., Baqi, Y., Muller, C.E., Rodrigues, A.L., Porciúncula, L.O., Chen, J.F., Tomé, A.R., Agostinho, P., Canas, P.M., Cunha, R.A., 2015. Caffeine acts through neuronal adenosine A_{2A} receptors to prevent mood and memory dysfunction triggered by chronic stress. Proc. Natl. Acad. Sci. U. S. A. 112, 7833–7838. https://doi.org/10.1073/pnas.1423088112.

Kim, J., Shin, W., 2014. How to do random allocation (randomization). Clin. Orthop. Surg. 6, 103–109. https://doi.org/10.4055/cios.2014.6.1.103.

Kishino, T., Lalande, M., Wagstaff, J., 1997. Ube3a/E6-AP mutations cause Angelman syndrome. Nat. Genet. 15, 70–73. https://doi.org/10.1038/ng0197-70.

Koyavski, L., Panov, J., Simchi, L., Rayi, P.R., Sharvit, L., Feuermann, Y., Kaphzan, H., 2019. Sex-dependent sensory phenotypes and related transcriptomic expression profiles are differentially affected by Angelman syndrome. Mol. Neurobiol. 56 (9), 5998–6016. https://doi.org/10.1007/s12035-019-1503-8.

Laurent, C., Burnouf, S., Ferry, B., Batalha, V.L., Coelho, J.E., Baqi, Y., Malik, E., Marciniak, E., Parrot, S., Van der Jeugd, A., Faivre, E., Flaten, V., Ledent, C., D'Hooge, R., Sergeant, N., Hamdane, M., Humez, S., Muller, C.E., Lopes, L.V., Buée, L., Blum, D., 2016. A_{2A} adenosine receptor deletion is protective in a mouse model of Tauopathy. Mol. Psychiatry 21, 149. https://doi.org/10.1038/mp.2014.151.

Li, P., Rial, D., Canas, P.M., Yoo, J.H., Li, W., Zhou, X., Wang, Y., van Westen, G.J., Payen, M.P., Augusto, E., Gonçalves, N., Tomé, A.R., Li, Z., Wu, Z., Hou, X., Zhou, Y., Jzerman, P., Boyden, E.S., Cunha, R.A., Qu, J., Chen, J.F., 2015. Optogenetic activation of intracellular adenosine A_{2A} receptor signaling in the hippocampus is sufficient to trigger CREB phosphorylation and impair memory. Mol. Psychiatry 20, 1339–1349. https://doi.org/10.1038/mp.2014.182.

Liu, Y., Johe, K., Sun, J., Hao, X., Wang, Y., Bi, X., Baudry, M., 2019. Enhancement of synaptic plasticity and reversal of impairments in motor and cognitive functions in a mouse model of Angelman syndrome by a small neurogenic molecule, NSI-189. Neuropharmacology 144, 337–344. https://doi.org/10.1016/j.neuropharm.2018.10.038.

Lopes, L.V., Halldner, L., Rebola, N., Johansson, B., Ledent, C., Chen, J.F., Fredholm, B.B., Cunha, R.A., 2004. Binding of the prototypical adenosine A_{2A} receptor agonist CGS 21680 to the cerebral cortex of adenosine A_1 and A_{2A} receptor knockout mice. Br. J. Pharmacol. 141, 1006–1014. https://doi.org/10.1038/sj.bjp.0705692.

Lopes, J.P., Morato, X., Souza, C., Pinhal, C., Machado, N.J., Canas, P.M., Silva, H.B., Stagljar, I., Gandia, J., Fernandez-Duenas, V., Lujan, R., Cunha, R.A., Ciruela, F., 2015. The role of Parkinson's disease-associated receptor GPR37 in the hippocampus: functional interplay with the adenosinergic system. J. Neurochem. 134, 135–146. https://doi.org/10.1111/jnc.13109.

Mabb, A.M., Judson, M.C., Zylka, M.J., Philpot, B.D., 2011. Angelman syndrome: insights into genomic imprinting and neurodevelopmental phenotypes. Trends Neurosci. 34, 293–303. https://doi.org/10.1016/j.tins.2011.04.001.

Maranga, C., Fernandes, T.G., Bekman, E., Teixeira da Rocha, S., 2020. Angelman syndrome: a journey through the brain. FEBS J. https://doi.org/10.1111/febs.15258.

Mardirossian, S., Rampon, C., Salvert, D., Fort, P., Sarda, N., 2009. Impaired hippocampal plasticity and altered neurogenesis in adult Ube3a maternal deficient mouse model for Angelman syndrome. Exp. Neurol. 220, 341–348. https://doi.org/10.1016/j.expneurol.2009.08.035.

Matos, M., Augusto, E., Santos-Rodrigues, A.D., Schwarzschild, M.A., Chen, J.F., Cunha, R.A., Agostinho, P., 2012. Adenosine A2A receptors modulate glutamate uptake in cultured astrocytes and gliosomes. Glia 60, 702–716. https://doi.org/10.1002/glia.22290.

Ménard, C., Quirion, R., 2012. Group 1 metabotropic glutamate receptor function and its regulation of learning and memory in the aging brain. Front. Pharmacol. 3, 182. https://doi.org/10.3389/fphar.2012.00182.

Morris, R.G., Garrud, P., Rawlins, J.N., O'Keefe, J., 1982. Place navigation impaired in rats with hippocampal lesions. Nature 297, 681–683. https://doi.org/10.1038/297681a0.

Mouro, F.M., Batalha, V.L., Ferreira, D.G., Coelho, J.E., Baqi, Y., Muller, C.E., Lopes, L.V., Ribeiro, J.A., Sebastião, A.M., 2017. Chronic and acute adenosine A_{2A} receptor blockade prevents long-term episodic memory disruption caused by acute cannabinoid CB_1 receptor activation. Neuropharmacology 117, 316–327. https://doi.org/10.1016/j.neuropharm.2017.02.021.

Musi, C.A., Agro, G., Buccarello, L., Camuso, S., Borsello, T., 2020. JNK signaling activation in the Ube3a maternal deficient mouse model: its specific inhibition prevents post-synaptic protein-enriched fraction alterations and cognitive deficits in Angelman Syndrome model. Neurobiol. Dis. 104812. https://doi.org/10.1016/j.nbd.2020.104812.

Pagnussat, N., Almeida, A.S., Marques, D.M., Nunes, F., Chenet, G.C., Botton, P.H., Mioranzza, S., Loss, C.M., Cunha, R.A., Porciúncula, L.O., 2015. Adenosine A_{2A} receptors are necessary and sufficient to trigger memory impairment in adult mice. Br. J. Pharmacol. 172, 3831–3845. https://doi.org/10.1111/bph.13180.

Quiroz, C., Luján, R., Uchigashima, M., Simões, A.P., Lerner, T.N., Borycz, J., Kachroo, A., Canas, P.M., Orru, M., Schwarzschild, M.A., Rosin, D.L., Kreitzer, A.C., Cunha, R.A., Watanabe, M., Ferré, S., 2009. Key modulatory role of presynaptic adenosine A2A receptors in cortical neurotransmission to the striatal direct pathway. ScientificWorldJournal 9, 1321–1344. https://doi.org/10.1100/tsw.2009.143.

Rebola, N., Canas, P.M., Oliveira, C.R., Cunha, R.A., 2005. Different synaptic and subsynaptic localization of adenosine A_{2A} receptors in the hippocampus and striatum of the rat. Neuroscience 132, 893–903. https://doi.org/10.1016/j.neuroscience.2005.01.014.

Reis, S.L., Silva, H.B., Almeida, M., Cunha, R.A., Simões, A.P., Canas, P.M., 2019. Adenosine A_1 and A_{2A} receptors differently control synaptic plasticity in the mouse dorsal and ventral hippocampus. J. Neurochem. 151, 227–237. https://doi.org/10.

1111/jnc.14816.
Rodrigues, R.J., Canas, P.M., Lopes, L.V., Oliveira, C.R., Cunha, R.A., 2008. Modification of adenosine modulation of acetylcholine release in the hippocampus of aged rats. Neurobiol Aging. 29, 1597–1601. https://doi.org/10.1016/j.neurobiolaging.2007.03.025.
Rogers, J., Churilov, L., Hannan, A.J., Renoir, T., 2017. Search strategy selection in the Morris water maze indicates allocentric map formation during learning that underpins spatial memory formation. Neurobiol. Learn. Mem. 139, 37–49. https://doi.org/10.1016/j.nlm.2016.12.007.
Schulte, G., Fredholm, B.B., 2003. Signalling from adenosine receptors to mitogen-activated protein kinases. Cell. Signal. 15, 813–827. https://doi.org/10.1016/S0898-6568(03)00058-5.
Sell, G.L., Margolis, S.S., 2015. From Ube3a to Angelman syndrome: a substrate perspective. Front. Neurosci. 9. https://doi.org/10.3389/fnins.2015.00322.
Shapiro, M., 2001. Plasticity, hippocampal place cells, and cognitive maps. Arch. Neurol. 58, 874–881. https://doi.org/10.1001/archneur.58.6.874.
Shi, S.Q., Bichell, T.J., Ihrie, R.A., Johnson, C.H., 2015. Ube3a imprinting impairs circadian robustness in Angelman syndrome models. Curr Biol. 25, 537–545. https://doi.org/10.1016/j.cub.2014.12.047.
Silva, A.C., Lemos, C., Gonçalves, F.Q., Pliássova, A.V., Machado, N.J., Silva, H.B., Canas, P.M., Cunha, R.A., Lopes, J.P., Agostinho, P., 2018. Blockade of adenosine A_{2A} receptors recovers early deficits of memory and plasticity in the triple transgenic mouse model of Alzheimer's disease. Neurobiol. Dis. 117, 72–81. https://doi.org/10.1016/j.nbd.2018.05.024.
Sonzogni, M., Wallaard, I., Santos, S.S., Kingma, J., du Mee, D., van Woerden, G.M., Elgersma, Y., 2018. A behavioral test battery for mouse models of Angelman syndrome: a powerful tool for testing drugs and novel Ube3a mutants. Mol. Autism 9. https://doi.org/10.1186/s13229-018-0231-7.
Stanford Behavioral & Functional Neuroscience Laboratory, 2007. "Standard Operating Procedure: Morris water maze." In, 1–11. Version 4.0.
Sun, J., Zhu, G., Liu, Y., Standley, S., Ji, A., Tunuguntla, R., Wang, Y., Claus, C., Luo, Y., Baudry, M., Bi, X., 2015. Ube3a regulates synaptic plasticity and learning and memory by controlling SK2 channel endocytosis. Cell Rep. 12, 449–461. https://doi.org/10.1016/j.celrep.2015.06.023.
Sun, J., Liu, Y., Tran, J., O'Neal, P., Baudry, M., Bi, X., 2016. mTORC1-S6K1 inhibition or mTORC2 activation improves hippocampal synaptic plasticity and learning in Angelman syndrome mice. Cell. Mol. Life Sci. 73, 4303–4314. https://doi.org/10.1007/s00018-016-2269-z.
Temido-Ferreira, M., Ferreira, D.G., Batalha, V.L., Marques-Morgado, I., Coelho, J.E., Pereira, P., Gomes, R., Pinto, A., Carvalho, S., Canas, P.M., Cuvelier, L., Buée-Scherrer, V., Faivre, E., Baqi, Y., Muller, C.E., Pimentel, J., Schiffmann, S.N., Buee, L., Bader, M., Outeiro, T.F., Blum, D., Cunha, R.A., Marie, H., Pousinha, P.A., Lopes, L.V., 2020. Age-related shift in LTD is dependent on neuronal adenosine A_{2A} receptors interplay with mGluR5 and NMDA receptors. Mol. Psychiatry 25, 1876–1900. https://doi.org/10.1038/s41380-018-0110-9.
Van der Jeugd, A., Ahmed, T., Burnouf, S., Belarbi, K., Hamdame, M., Grosjean, M.E., Humez, S., Balschun, D., Blum, D., Buée, L., D'Hooge, R., 2011. Hippocampal tauopathy in tau transgenic mice coincides with impaired hippocampus-dependent learning and memory, and attenuated late-phase long-term depression of synaptic transmission. Neurobiol. Learn. Mem. 95, 296–304. https://doi.org/10.1016/j.nlm.2010.12.005.
van Woerden, G.M., Harris, K.D., Hojjati, M.R., Gustin, R.M., Qiu, S., de Avila Freire, R., Jiang, Y.H., Elgersma, Y., Weeber, E.J., 2007. Rescue of neurological deficits in a mouse model for Angelman syndrome by reduction of alphaCaMKII inhibitory phosphorylation. Nat. Neurosci. 10, 280–282. https://doi.org/10.1038/nn1845.
Viana da Silva, S., Haberl, M.G., Zhang, P., Bethge, P., Lemos, C., Gonçalves, N., Gorlewicz, A., Malezieux, M., Gonçalves, F.Q., Grosjean, N., Blanchet, C., Frick, A., Nagerl, U.V., Cunha, R.A., Mulle, C., 2016. Early synaptic deficits in the APP/PS1 mouse model of Alzheimer's disease involve neuronal adenosine A_{2A} receptors. Nat. Commun. 7, 11915. https://doi.org/10.1038/ncomms11915.
Vorhees, C.V., Williams, M.T., 2006. Morris water maze: procedures for assessing spatial and related forms of learning and memory. Nat. Protoc. 1, 848–858. https://doi.org/10.1038/nprot.2006.116.